

Commissioning of Particle ID at ATLAS and CMS with Early LHC Data

T. Berger-Hryn'ova
CERN, 1211 Geneve 23, Switzerland
on behalf of the ATLAS and CMS collaborations

This paper describes latest results on lepton (electron, muon and tau) and photon particle identification at the ATLAS and CMS experiments, with emphasis on how the particle identification can be validated and its performance determined using early LHC data.

1. INTRODUCTION

ATLAS and CMS are the two general-purpose experiments, which have recently completed installation at the CERN Large Hadron Collider (LHC). Many physics processes which are currently out of reach at existing colliders will become accessible at the LHC. These processes range from the production of scalar Higgs bosons or of new vector gauge bosons to that of supersymmetric particles or of TeV-scale resonances resulting from presence of large extra-dimensions. Charged leptons often provide distinctive signatures for such new processes, but they also appear in the final state of many standard-model (SM) processes involving electroweak (EW) bosons or top quarks. These SM processes constitute the dominant background to new signals and therefore need to be well understood. They will also be used as calibration processes to understand in detail the performance of the detector.

Thus, lepton (and photon) identification is very important for the physics program of ATLAS and CMS. With a bunch-crossing rate of 40 MHz at design luminosity, of which only 200-300 Hz are planned to be recorded to mass storage, particle identification is extremely important also at the trigger level and it will be crucial to commission it as early as possible.

The main data samples used to understand the detector performance and the lepton identification are well-known EW processes, such as $Z \rightarrow ll$ and $W \rightarrow l\nu$. They provide important benchmark channels for calibration, alignment and monitoring of the detector performance. However, at the expected start-up luminosities of $10^{31} - 10^{32} \text{ cm}^{-2}\text{s}^{-1}$, the total bandwidth for EW processes will be below 1 Hz, compared to a few tens of Hz expected at $10^{33} \text{ cm}^{-2}\text{s}^{-1}$, which will severely limit the statistics of such samples. On the other hand, at these lower luminosities, the triggers can be operated with lower E_T -thresholds than those planned for the LHC design luminosity. This would potentially give access to other more abundant data samples, such as direct J/ψ , Υ , etc.

This paper describes the commissioning strategies in the following order: identifications of photons, electrons, muons and τ -leptons. For a detailed description of the ATLAS and CMS detectors and of their current commissioning status please see Refs. [1, 2, 3].

2. Photons and Electrons

Photon and electron identification in ATLAS and CMS is extremely challenging: the electron to jet ratio is $\approx 10^{-5}$ at 40 GeV. Photon and electron reconstruction in both experiments starts by the detection of clusters in the electromagnetic calorimeters. Electron candidates are also required to have an inner-detector track loosely matched to the cluster. In ATLAS, there is also a dedicated low- p_T electron reconstruction algorithm, which extrapolates inner-detector tracks to the EM calorimeter. The reconstruction of photons and electrons is quite challenging in both experiments because of the $\approx 0.4 - 2.4X_0$ of material in the inner detectors. For example, in ATLAS, electrons with $E_T = 25$ GeV lose on average 30 - 60% of their energy before reaching the EM calorimeter, and between 10 and

60% of photons convert into an electron-positron pair. For a more detailed description of the electron and photon reconstruction in ATLAS and CMS, see Ref. [4].

Despite some significant differences in detector technologies and intrinsic performance (e.g. the sampling LAr EM calorimeter of ATLAS and the homogeneous PbWO₄ crystal EM calorimeter of CMS), the performances expected for electrons and photons are similar for both experiments in terms of efficiency and accuracy. For example electrons of 50 GeV energy are expected to be measured with a 1.5 – 2.5% energy resolution in ATLAS and with a 2% energy resolution in CMS. Photons with a 100 GeV energy are expected to be measured with a 1.0 – 1.5% energy resolution in ATLAS. For 70% of the photons which do not convert too early in the tracker, the energy resolution is expected to be better in CMS, e.g. $\approx 0.8\%$ due to the superior intrinsic accuracy of the crystal calorimeter.

Very high rejection of the large background from hadronic jets is another important aspect of electron and photon identification at the LHC. In ATLAS, for a photon reconstruction efficiency of 85%, one can obtain a jet rejection of ≈ 10000 averaged over all jets types (quark and gluon jets). For tight electron selection and for $E_T > 20$ GeV, the identification efficiency of isolated electrons from Z decays is 65% (it drops to $\approx 25\%$ for non-isolated electrons from b/c -decays) with a jet rejection of $\approx 10^5$. After such tight electron selection of inclusive electrons with $E_T > 20$ GeV the remaining sample is expected to contain 10% of isolated and 65% of non-isolated electrons, with the remaining 25% expected to consist of residual background from hadronic jets dominated by charged hadrons. The use of multivariate methods improves the rejection by 50% for a fixed efficiency or improves the efficiency by 5 – 10% for a fixed rejection.

Obviously, those expected performances will have to be validated with real data. Both experiments are planning to use the early data to understand the tracker (alignment, material distribution), to perform detailed intrinsic calibrations of the EM calorimeters, as well as to measure the trigger efficiency. All these aspects are crucial to obtain a detailed understanding of the electron and photon identification performances.

2.1. Photons

Photon identification is particularly challenging, since there do not exist any prominent di-photon resonances at high mass which could be used for calibration and efficiency measurement purposes. Thus, the understanding of photon identification in the early data will have to rely heavily on the understanding of electrons, using simulations to account for the small differences between them. As soon as a few fb^{-1} of data become available $Z \rightarrow ee\gamma$ and $Z \rightarrow \mu\mu\gamma$ decays will be used to improve the understanding of high- p_T photons further. In CMS the achievable statistical error on the photon efficiency is estimated to be 0.1% with 1fb^{-1} of data. At much lower p_T , one could use π^0 and η decays to $\gamma\gamma$ to understand photon identification in early data. Converted photons from π^0/η decays will be extremely useful to obtain a detailed mapping of the tracker material. This is strongly correlated with a precise EM calorimeter inter-calibration, as discussed below.

2.2. Electrons

A detailed understanding of electron reconstruction and identification at the LHC will rely strongly on the presence of “standard candles”, such as the Z and W resonances, for the calibration of the energy scale, for the EM inter-calibration, and for a precise understanding of the detector and trigger efficiencies, etc.

Both experiments are planning to use the precise knowledge of the Z mass to perform an accurate EM calorimeter inter-calibration. Since the ATLAS EM calorimeter is locally very uniform by construction, only an inter-calibration of large regions is required. The initial spread from region to region is conservatively assumed to be approximately 1.5 – 2%. Provided the material distribution in front of the EM calorimeter is well-understood, the specified inter-calibration precision of 0.7% between regions of 0.2×0.4 in $\eta \times \phi$ can be achieved in the case of ATLAS with 100pb^{-1} of data. In the CMS EM calorimeter, the energy response may vary with a spread of 3 – 4% from crystal to crystal, and therefore a precise inter-crystal calibration has to be performed. Initially, single-jet triggers will be used to

inter-calibrate ϕ rings at fixed η with an accuracy of a few percent, as is shown in Fig. 1. For the final precision the $Z \rightarrow ee$ sample corresponding to $\approx 2 \text{ fb}^{-1}$ of data is needed to reach the specified target of 0.5%.

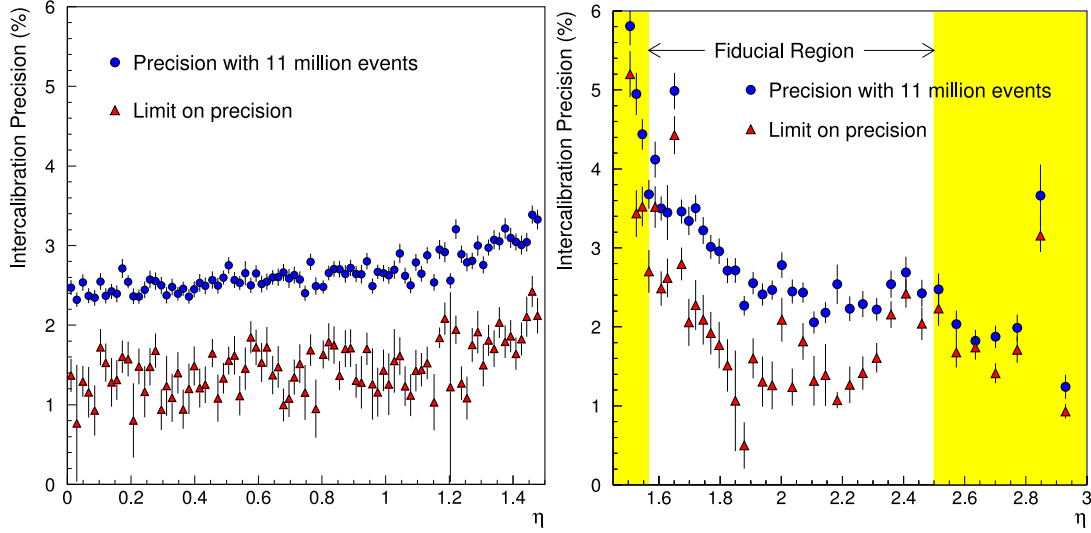


Figure 1: CMS inter-calibration precision in barrel (left) and endcap (right) which can be obtained with 11 million Level-1 jet trigger events and the limit on the inter-calibration precision due to tracker material inhomogeneity as a function of η (from Ref. [5]).

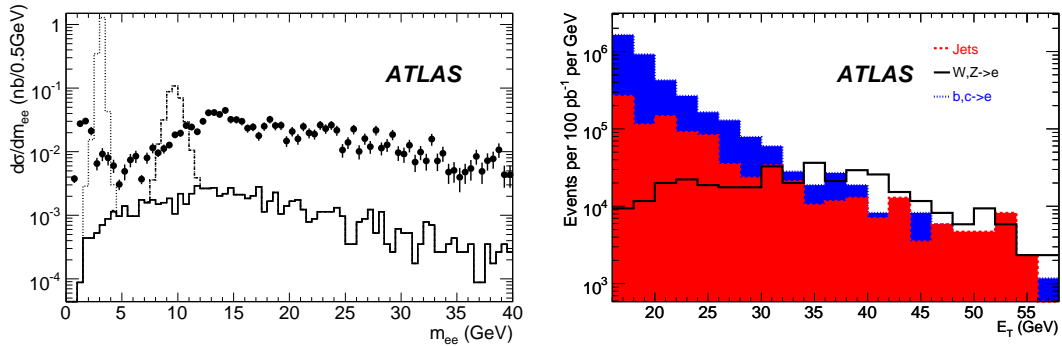


Figure 2: (Left) Expected differential cross-section for low-mass electron pairs using the dedicated ATLAS low- p_T dielectron trigger. Shown is the invariant di-electron mass distribution reconstructed using tracks for $J/\psi \rightarrow ee$ decays (dotted histogram), $\Upsilon \rightarrow ee$ decays (dashed histogram) and Drell-Yan production (full histogram). Also shown is the expected background (full circles). (Right) Expected differential rates in ATLAS as a function of electron E_T for 100 pb^{-1} of data and for electrons satisfying tight single-electron selection. Shown are the isolated electrons from W and Z decays (solid histogram), the non-isolated electrons from $b, c \rightarrow e$ decays (light gray/red histogram), and the estimated QCD background (dark gray/blue histogram).

In ATLAS, specific triggers have been implemented for electron pairs from direct J/ψ and Υ production, which are expected to provide about 200k and 50k events respectively for 100 pb^{-1} of data (compared to 50k of events on the Z resonance). The expected signal and background dielectron mass distributions after tight electron selection are shown in Fig. 2 (left). The obtained J/ψ sample can also be used for the calorimeter inter-calibration and preliminary studies [6] show that a precision of $\approx 0.6\%$ may be achieved. In addition to a cross-check on the inter-calibration result obtained using the Z resonance, the J/ψ and Υ samples will also provide an in-situ check of the linearity of the EM calorimeter response as a function of electron energy. The additional electron identification capabilities provided

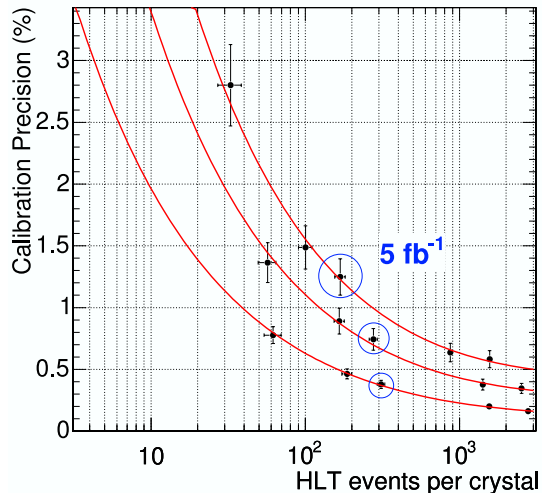


Figure 3: CMS inter-calibration precision as a function of HLT events per crystal for different η regions. Upper curve: last 10 crystals in the EM calorimeter barrel ($1.305 < \eta < 1.479$), middle curve: 10 crystals in the middle EM calorimeter barrel ($0.783 < |\eta| < 0.957$), lower curve: the first 15 crystals in the EM calorimeter barrel ($0.0 < |\eta| < 0.261$). The third point on each line gives the precision for 5 fb^{-1} of integrated luminosity (from Ref. [5]).

by the ATLAS transition radiation detector may turn out to be crucial to identify low-energy electrons from J/ψ and Υ decays, since they are usually not as well isolated as those from Z decay and since the charged-pion combinatorial background is very large.

Isolated single electrons from $W \rightarrow e\nu$ decays will provide further information for tracker-EM calorimeter inter-calibration by comparing the energy deposited in the calorimeter to the track momentum measurement. As shown in Fig. 3, an inter-calibration precision of 0.5–1.5% may be achieved in CMS with 5 fb^{-1} of data. Non-isolated electrons from $b, c \rightarrow e$ decays could also be used for this purpose during the early data-taking while the single-electron trigger thresholds are low. As one can see from Fig. 2 (right), these decays are dominant for $E_T < 35 \text{ GeV}$ and they should provide ten times more electrons with $E_T > 10 \text{ GeV}$ than those from W decay.

Since the trigger efficiency represents a fundamental ingredient of any physics analysis, it must be verified as independently as possible from simulations and as a function of the LHC physics and detector operation conditions. One of the most widely spread techniques under study is the “tag-and-probe” method, where an event is triggered by one of the electrons in a $Z \rightarrow ee$ decay and the efficiency to trigger the other electron is measured using offline information. With 100 pb^{-1} of data, one will measure the trigger efficiency for electrons of $E_T > 20 \text{ GeV}$ with a statistical accuracy of approximately 0.2% [2, 7].

3. Muons

Muons are identified through matching reconstructed tracks in the inner tracker and the muon spectrometer. ATLAS and CMS follow complementary concepts of muon detection. ATLAS has an instrumented air-toroid magnetic system serving as a stand-alone high-precision muon spectrometer. CMS relies on high bending power and momentum resolution in the inner tracker, and on the iron yoke used for the return of its solenoidal magnetic field. The iron yoke is instrumented with chambers used for muon identification and triggering. Stand-alone muon tracks can be reconstructed, but in order to obtain a precise momentum measurement it is essential to combine the inner-tracker information with that from the muon chambers.

The momentum resolution of the ATLAS and CMS detectors are shown in Fig. 4. Whereas the stand-alone muon resolution is fairly uniform over most of the $\eta - \phi$ plane in ATLAS as is shown in Fig. 5(left) with optimal resolution

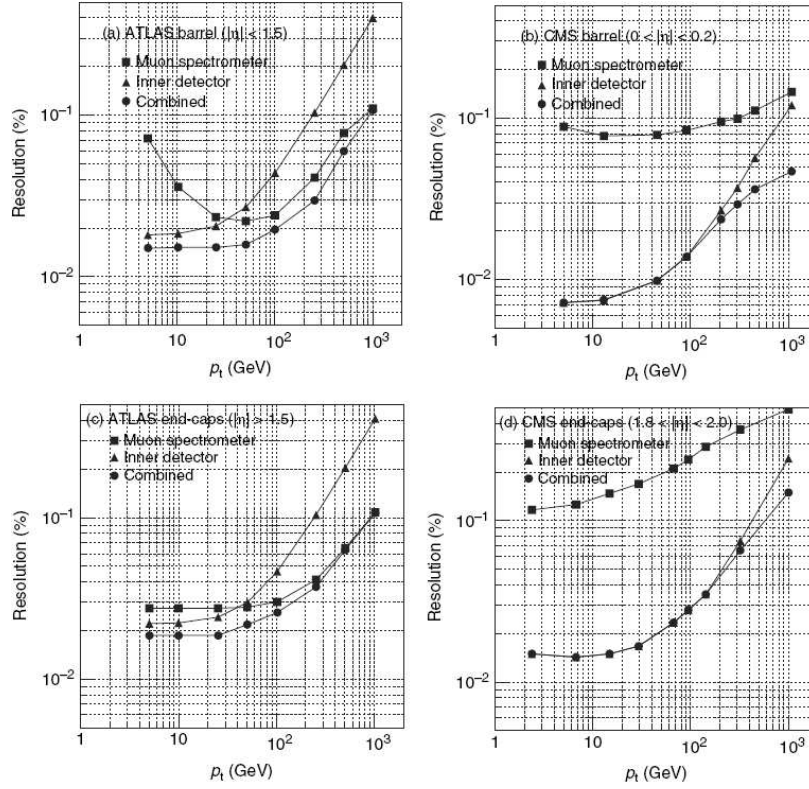


Figure 4: Relative momentum resolution as a function of the muon transverse momentum showing the stand-alone resolution of muon systems, the stand-alone resolution of the inner tracker and the combined resolution: (a) and (c) in ATLAS for $|\eta| < 1.5$ and $|\eta| > 1.5$, respectively; (b) and (d) in CMS for $0 < |\eta| < 0.2$ and $1.8 < |\eta| < 2.0$, respectively. From Ref. [8].

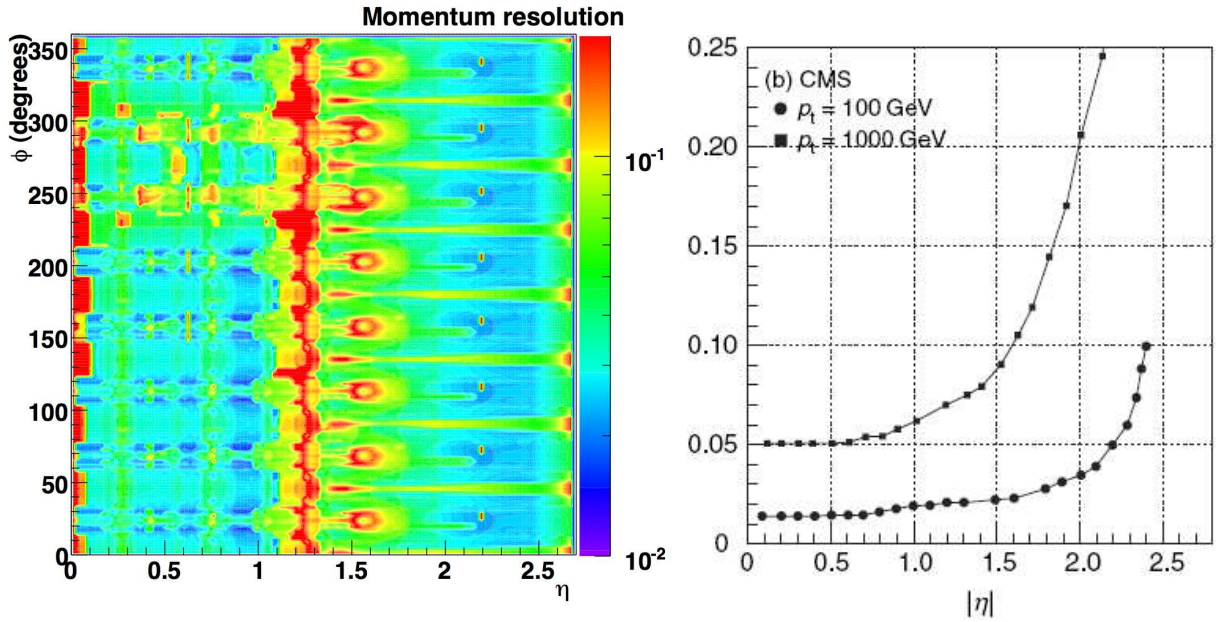


Figure 5: (left) For muons with $p_T = 100$ GeV, expected fractional stand-alone momentum resolution in ATLAS as a function of ϕ and $|\eta|$ (from Ref. [2]). No momentum measurement is possible at $|\eta| < 0.1$ over most of the azimuth, nor at $|\eta| = 1.3$ because of holes in the acceptance of the muon spectrometer. (right) Relative momentum resolution for combined muon reconstruction in CMS as a function of $|\eta|$ for two different values of transverse momentum (from Ref. [8]).

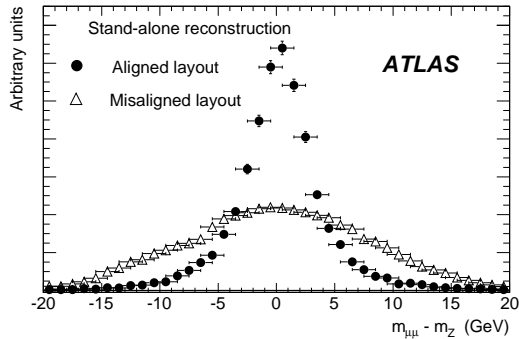


Figure 6: Difference between reconstructed and true dimuon mass from $Z \rightarrow \mu\mu$ decays, as obtained from an aligned and a misaligned muon spectrometer in ATLAS.

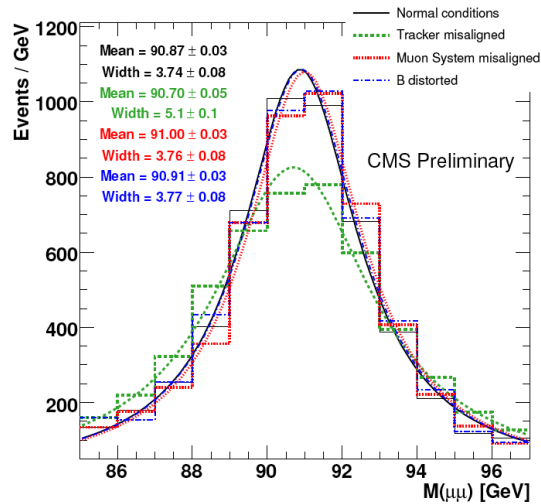


Figure 7: Effect on the reconstructed Z boson mass in CMS of the misalignment and of the uncertainties on the magnetic field after the muon scale calibration. Fits are sums of a Lorentzian and a linear function. See Ref. [10] for details.

achieved at 100 GeV, the resolution degrades at high η in CMS because of the limited coverage of the solenoid (Fig. 5(right)). The resolution of the combined measurement in the barrel region is slightly better in CMS owing to the higher precision of the measurement in the tracking system, whereas the reverse is true in the end-cap region owing to the better coverage of the ATLAS muon spectrometer at higher rapidities.

The muon reconstruction efficiencies are high (above 96%) for both experiments with fake rates of about 1% from neutron background at the LHC design luminosity, see Ref. [9] for details. The combination of inner tracker, calorimeter and muon spectrometer measurements is required in ATLAS to minimize inefficiencies due to holes in the coverage of the muon spectrometer system as is shown in Fig. 5.

The large expected rates of $Z \rightarrow \mu\mu$ decays provide an excellent tool to untangle various effects which might lead to distortions of the measured dimuon invariant mass spectrum. One example is shown in Fig. 6 for ATLAS stand-alone muon measurements, where the performance obtained with a misaligned layout (with random displacements of 1 mm and a random rotations of 1 mrad of each chamber in the muon spectrometer) is compared to that expected from a perfectly aligned layout. The large assumed misalignments lead to an increase in the fitted Gaussian resolution of the dimuon reconstructed invariant mass from 2.5 GeV to 8 GeV. Similar distortions including a potential shift in the mean of the peak could be caused by muon momentum scale biases and uncertainties in the initial knowledge of the magnetic field as is shown in Fig. 7.

The muon reconstruction and identification efficiency will also be measured from data using $Z \rightarrow \mu\mu$ decays and

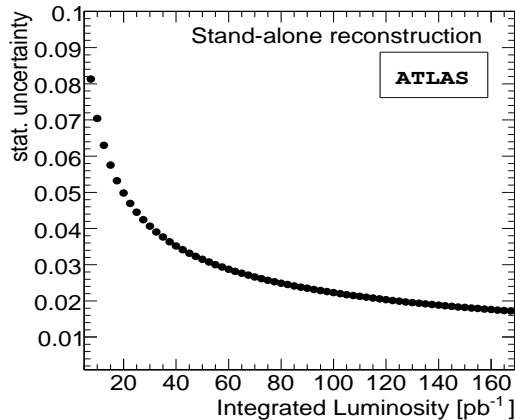


Figure 8: Average statistical error expected for the measured muon reconstruction efficiency in ATLAS for 320 regions of the muon spectrometer as a function of integrated luminosity.

the tag-and-probe method described in Section 2.2, with similar results expected in terms of the accuracy of the measurement. This type of analysis can be extended to study efficiency with increasing granularity as the integrated luminosity increases, in particular as a function of η and ϕ . An example of the expected statistical uncertainty on the reconstruction efficiency in the muon spectrometer, averaged over 320 regions in the $\eta - \phi$ plane, is shown in Fig. 8. Other resonances, such as J/ψ and Υ , could also be used for this analysis at lower initial luminosities. The expected rates for 100 pb^{-1} of data in ATLAS/CMS are 1.6 M J/ψ , 300k Υ and 60k Z -decays.

4. τ -leptons

The τ -lepton is the heaviest lepton observed to-date and it decays to electrons, muons and hadrons. This section concentrates on the identification on τ -leptons decaying hadronically. They are reconstructed by matching narrow calorimeter clusters with a small number of tracks reconstructed in the inner tracker.

One will need to demonstrate that the observed signals from $W \rightarrow \tau\nu$ and $Z \rightarrow \tau\tau$ decays are in agreement with fundamental properties of the τ -lepton (e.g. visible mass and decay length measurement for three-prong decays). One of the distinctive features of hadronic τ decays is the track multiplicity spectrum shown in Fig. 9 for $Z \rightarrow \tau\tau$ decays (left) and for jets (right). The distributions are shown after the reconstruction step, after a cut-based identification algorithm and finally after applying a multi-variate discrimination technique using a neural network. Figure 9 shows that the signal track multiplicity distributions do not depend strongly on the reconstruction and identification cuts used. It also shows that the track multiplicity in the QCD jet sample is quite different from that in the signal sample and that the candidates with track multiplicity above three may be used to normalize the background. This would allow a reasonably precise calibration of the performance of the τ -identification algorithms using real data, provided the rejection against QCD jets is proven to be sufficient to extract clean signals in the single-prong and three-prong categories.

Triggering on hadronic τ -decays is extremely challenging because of the huge backgrounds from hadronic jets and of the requirement to bias minimally the track multiplicity spectrum. The τ -triggers increase the discovery potential for many physics channels and in rare cases provide the only trigger, e.g. $W \rightarrow \tau\nu$ decays.

$W \rightarrow \tau\nu$ decays provide the most abundant source of τ -leptons in SM processes. Due to trigger rate limitations, they are only expected to be accessible at initial low luminosities. The dominant background for it arises from hadronic jets and the signal-to-background ratio is expected to be a factor of ten worse than that observed at the TeVatron. Preliminary studies show that it is possible to reach a signal-to-background ratio of about three in this channel with ≈ 1500 $W \rightarrow \tau\nu$ signal events for 100 pb^{-1} of data. The goal of such an analysis would be to show

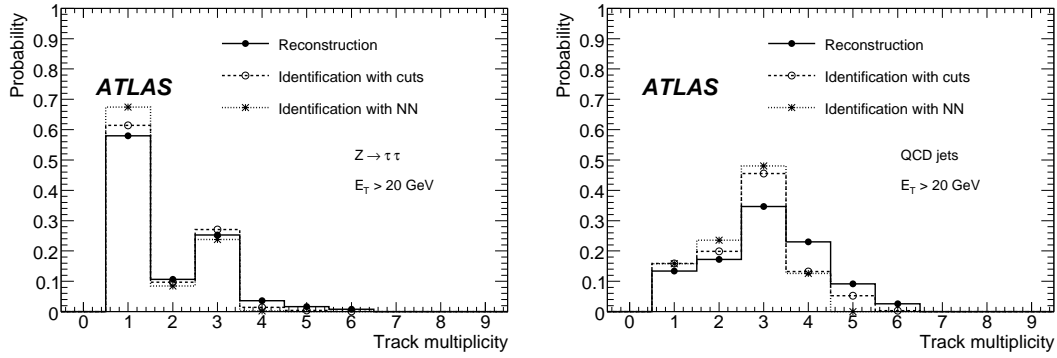


Figure 9: Track multiplicity distributions expected in ATLAS for hadronic τ -decays (left) and for the background from hadronic jets (right), for τ -candidates with visible transverse energy above 20 GeV reconstructed using a track-based τ -identification algorithm. The distributions are shown after reconstruction, after cut-based identification, and finally after applying a neural network discrimination technique, resulting in an efficiency of 30% for the signal.

track-multiplicity spectrum of identified τ -leptons as a proof of τ -lepton observability.

The most interesting SM sample is that from $Z \rightarrow \tau\tau$ decays. Although the expected rate is ten times less than $W \rightarrow \tau\nu$ decays, this process exhibits a more interesting topology and is easily triggered by requiring a single lepton. Same-sign events which are nearly signal-free will be used to control the dominant QCD background in the signal-enriched opposite-sign events. The goal of this analysis is to set τ energy scale from the excess of signal events in the invariant mass of the visible decay products. The complete Z invariant mass can be also reconstructed in the collinear approximation. Preliminary studies from ATLAS expect to see about 520 signal events and 85 background events in 100pb^{-1} . The visible decay mass could be used to determine the τ energy scale with a precision of 3% (taking into account only statistical errors). Also assuming τ s are well-calibrated and using additional selection (≈ 200 signal and 20 background events remaining) and the collinear approximation, one could determine E_T^{miss} scale with 3% statistical precision. One should note that the E_T^{miss} scale could be more easily understood with $W \rightarrow e(\mu)\nu$ events.

5. Acknowledgments

The author would like to thank Daniel Froidevaux, Pascal Vanlaer, Oliver Kortner, Martijn Mulders and Elzbieta Richter-Was for the fruitful discussions and exchanges during this work.

References

- [1] J. Thomas, Commissioning of ATLAS, Proceedings of 19th Hadron Collider Physics Symposium (HCP 2008), this volume, Galena, IL, USA.
- [2] The ATLAS Experiment at the CERN Large Hadron Collider, the ATLAS Collaboration, G Aad *et al.*, JINST 3 S08003 (2008).
- [3] L. Malgeri, Commissioning of CMS, Proceedings of 19th Hadron Collider Physics Symposium (HCP 2008), this volume, Galena, IL, USA; The CMS experiment at the CERN LHC, the CMS Collaboration, S Chatrchyan *et al.*, JINST 3 S08004 (2008).
- [4] C. Charlot, Electron/Photon Identification in ATLAS and CMS, Proceedings of 17th Hadron Collider Physics Symposium (HCP 2006) [arXiv:0709.2479].
- [5] CMS Physics TDR vol. 1, CERN/LHCC 2006-001.

- [6] F. Derue, A. Kaczmarzka, Ph. Schwemling, Reconstruction of DC1 $J/\psi \rightarrow ee$ decays and use of the low energy calibration of the ATLAS electromagnetic calorimeter, 2006, ATL-PHYS-PUB-2006-004.
- [7] G.Daskalakis *et al.*, Measuring electron efficiencies at CMS with early data, CMS EGM-07-001-PAS.
- [8] F. Ragusa and L. Rolandi, Tracking at LHC, New J. Phys. 9 (2007) 336.
- [9] O. Kortner, Muon Identification in ATLAS and CMS, Proceedings of 17th Hadron Collider Physics Symposium (HCP 2006) [arXiv:0707.0905].
- [10] The CMS Collaboration, Towards a measurement of the inclusive $W \rightarrow \mu\nu$ and $Z \rightarrow \mu\mu$ cross sections in pp collisions at $\sqrt{s} = 14$ TeV, CMS PAS 2007/002.